

SUPPLEMENT TO “LIBERATION TECHNOLOGY: MOBILE PHONES AND
POLITICAL MOBILIZATION IN AFRICA”
(*Econometrica*, Vol. 88, No. 2, March 2020, 533–567)

MARCO MANACORDA
School of Economics and Finance, Queen Mary University of London

ANDREA TESEI
School of Economics and Finance, Queen Mary University of London

APPENDIX

A.1. *Theory Appendix*

A.1.1. *Setup*

WE CONSIDER a network of individuals characterized by the distribution $P(d)$ ($d = 0, 1, \dots, D$) of the number d of neighbors or degree, where $\sum_{d=0}^D P(d) = 1$. We regard mobile phones as increasing the number of neighbors and, as a result, increasing the density of the network. We revert to a more formal definition of network density below.

Each agent i has the choice between taking action 0, the status quo (in the present case, not protesting), or action 1 (in the present case, protesting).

We denote the utility of an agent of degree d_i from taking action 1 relative to action 0 when he expects his neighbors to choose action 1 with probability \bar{y}_{-i} by $v_i = v(d_i, \bar{y}_{-i})$. We follow others in the literature (e.g., Granovetter (1978), Jackson and Yariv (2007)) and assume that agents' decisions are characterized by strategic complementarities, that is, that the utility of agent i from taking action 1 is nondecreasing in \bar{y}_{-i} :

$$\frac{\partial v_i}{\partial \bar{y}_{-i}} \geq 0. \tag{A.1}$$

Each agent i has a cost of taking action 1, which we denote by c_i . We follow others in the literature by assuming that the opportunity cost of participating is higher when the economy improves. An alternative interpretation for this assumption is that reasons for grievance, and hence the incentives to protest, increase during bad economic times. We also assume that this cost can vary as a function of an individual's degree d_i . In formulas, we assume that $c_i = c(d_i, \Delta\text{GDP}) + \epsilon_i$, where ϵ_i is an error term that we assume independent of d_i , and with cumulative distribution function (c.d.f.) $H(\cdot)$ and

$$\frac{\partial c_i}{\partial \Delta\text{GDP}} \geq 0. \tag{A.2}$$

We follow Jackson and Yariv (2007) and assume for simplicity that ϵ is uniformly distributed. From the above discussion, it follows that the probability y_i that an agent i of degree d_i decides to join a protest given that his neighbors protest with probability \bar{y}_{-i} is

$$y_i = H(v_i - c_i). \tag{A.3}$$

Marco Manacorda: m.manacorda@qmul.ac.uk
Andrea Tesei: a.tesei@qmul.ac.uk

A.1.2. Equilibrium

We assume that each agent has limited information about the structure of the network: he only knows his own degree d_i and cost c_i and the overall distribution of degrees in the population $P(d)$. The play is symmetric in the sense that every agent perceives the distribution of plays of each of his neighbors to be independent and to correspond to the population distribution of plays.

Individuals iterate over neighbors' best responses given the probability distribution of the neighbors' degrees. Under the above hypotheses, an equilibrium for the game exists. In particular, at the equilibrium, the fraction of individuals participating, \bar{y} , is defined by the solution to the equation

$$\bar{y} = \phi(\bar{y}) := \sum_{d=0}^D \tilde{P}(d) H(v(d, \bar{y}) - c(d, \Delta\text{GDP})), \quad (\text{A.4})$$

where $\tilde{P}(d) = \frac{P(d)d}{E[d]}$ denotes the probability that a random neighbor is of degree d . The equilibrium condition effectively states that individuals' best responses are mutually consistent, that is, that the probability that a randomly chosen neighbor chooses action 1 (the left hand side term) equals the expectation that a random best responding neighbor chooses action 1 (the right hand side term). Although both stable and unstable equilibria are possible, for convenience we focus on the stable equilibrium. Again following [Jackson and Yariv \(2007\)](#), at the stable equilibrium it must be true that

$$\frac{\partial \phi(\cdot)}{\partial \bar{y}} < 1. \quad (\text{A.5})$$

A.1.3. Participation and the State of the Economy

We start by performing comparative statics on the equilibrium of the model in response to changes in the state of the economy ΔGDP .

From the definition of y_i , note that, conditional on the state of the economy and the agent's degree, around the equilibrium, individuals will be more likely to participate the higher is the fraction of other individuals participating, that is,

$$\frac{\partial y_i}{\partial \bar{y}} \Big|_{d_i, \Delta\text{GDP}} \geq 0. \quad (\text{A.6})$$

In addition, each individual's probability of participation will increase (decrease) as the state of the economy deteriorates (improves):

$$\frac{\partial y_i}{\partial \Delta\text{GDP}} \Big|_{d_i, \bar{y}} \leq 0. \quad (\text{A.7})$$

Note that equation (A.7) refers to an individual's propensity to participate in response to changes in the state of the economy *conditional* on the individuals' degree and the overall fraction of individuals participating, where the latter is itself a variable affected by economic conditions. In particular, one can show that this fraction increases (decreases)

as the state of the economy deteriorates (improves). From (A.4),

$$\frac{d\bar{y}}{d\Delta\text{GDP}} = \frac{\frac{\partial\phi(\cdot)}{\partial\Delta\text{GDP}}}{1 - \frac{\partial\phi(\cdot)}{\partial\bar{y}}} = \frac{\sum_{d=1}^D \tilde{P}(d) \frac{\partial H(\cdot)}{\partial\Delta\text{GDP}}}{1 - \sum_{d=1}^D \tilde{P}(d) \frac{\partial H(\cdot)}{\partial\bar{y}}} \leq 0, \quad (\text{A.8})$$

where the last inequality follows from the fact that, at the equilibrium, the numerator in (A.8) is negative (from equation (A.7)), while the denominator is positive (from equation (A.5)).

The intuition for this result is straightforward. Worse economic conditions mechanically raise each individual's propensity to protest (equation (A.7)). This raises protest participation and hence increases the fraction of those participating (this is the numerator of equation (A.8)). Strategic complementarities generate an additional effect as individuals iterate over their neighbors' best responses, knowing that everybody else will be more likely to participate and to know that everybody else will know, etcetera (this is the denominator of equation (A.8)). This mechanism further enhances the positive effect of recessions on the incidence of protests.

A.1.4. Differential Responses Based on the Density of the Network

We extend our analysis to study how economic conditions have a different impact on the probability of protesting depending on individuals' degree and the "density" of the network, that is, the distribution of degrees.

We make two additional assumptions:

$$\frac{\partial^2 c_i}{\partial\Delta\text{GDP}\partial d_i} \geq 0, \quad (\text{A.9})$$

$$\frac{\partial^2 v_i}{\partial\bar{y}_{-i}\partial d_i} \geq 0. \quad (\text{A.10})$$

Equation (A.9) states that the opportunity cost of participating responds more to the state of the economic cycle the higher the agent's degree. We take this assumption to reflect the circumstance that, compared to individuals with no mobile phones, those with mobile phones (i.e., those with higher degree) experience greater decreases (increases) in the cost of participation when the economy deteriorates (improves). One explanation for this is that individuals with mobile phones are more likely to correctly perceive the actual state of the economy due to the unadulterated nature of the information they are able to access. We label this mechanism *enhanced information*. An alternative explanation is that mobile phones are complementary to aggregate economic growth in determining one's productivity so the opportunity cost of protests varies differentially for those with and without mobile phones along the cycle. We attempt to investigate empirically these different explanations in Table IV in the paper.

Equation (A.10) states that the increase in utility from participation in response to a given increase in the fraction of neighbors participating is higher for those with mobile phones compared to those with no mobile phones. One way to rationalize this assumption is that mobile phones can help a person to better coordinate with other protesters, which

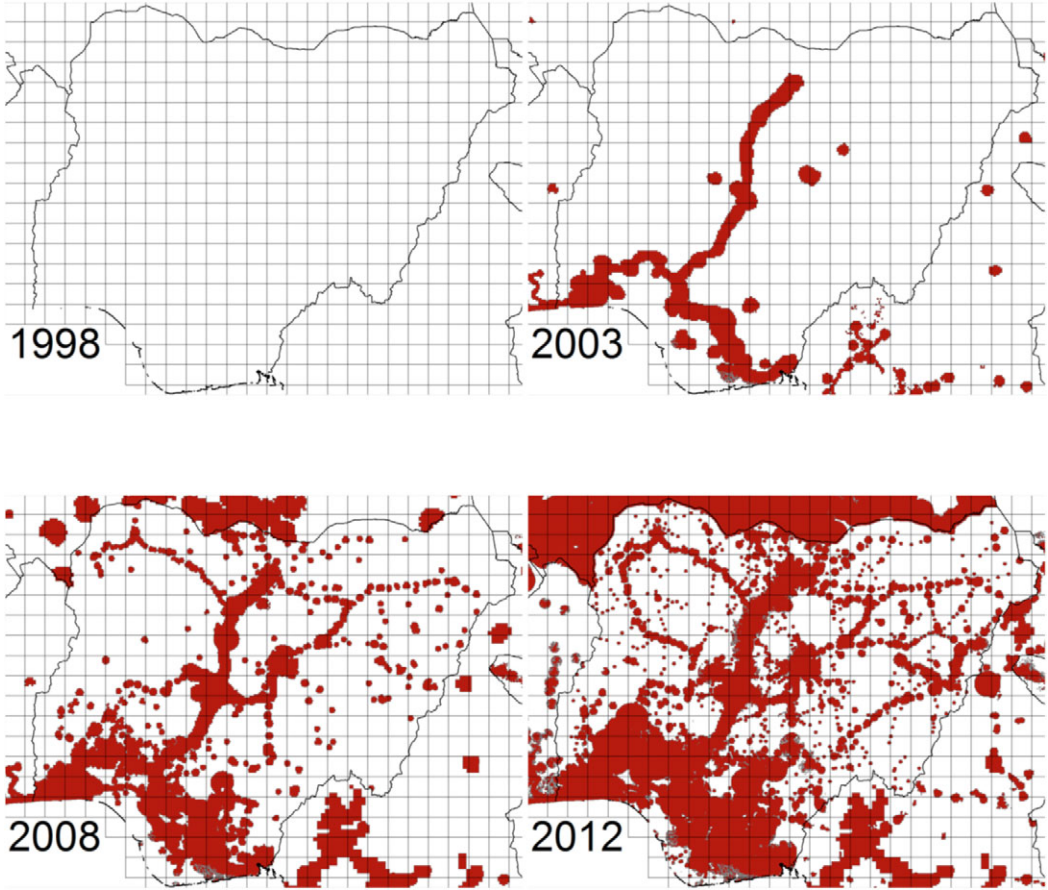


FIGURE A.1.—Mobile phone diffusion: Nigeria 1998–2012. The figure reports the spread of mobile phone coverage in Nigeria between 1998 and 2012 at 5-year intervals. Source: GSMA.

results in a higher increase in utility in response to an increase in the fraction of neighbors participating. We label this mechanism *enhanced coordination*.

The implications of these assumptions for individual behavior can be easily derived. Under (A.9) and (A.10),

$$\frac{\partial^2 y_i}{\partial \Delta \text{GDP} \partial d_i} \leq 0. \quad (\text{A.11})$$

This means that individual i 's probability of participation increases more in response to a deterioration in economic conditions the higher is this individual's number of connections, and

$$\frac{\partial^2 y_i}{\partial \bar{y} \partial d_i} \geq 0. \quad (\text{A.12})$$

Equation (A.12) states that the effect of changes in the fraction of individuals participating on each individual's probability of participation increases with his number of connections.

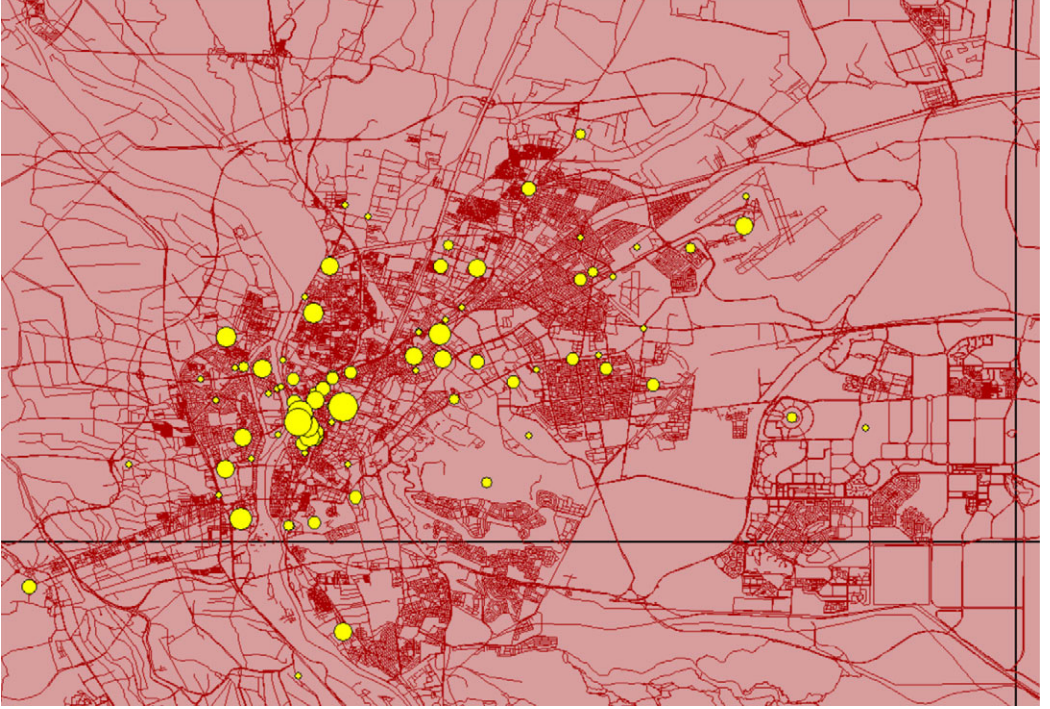


FIGURE A.2.—Geolocated protest events: Cairo 2011. The figure reports the occurrence of protests in Cairo in 2011 by location. Larger dots correspond to more days of protests in a certain location. Source: GDELT.

To understand how the density of the network affects the overall fraction of individuals participating, we define density in terms of first order stochastic dominance (FOSD). Given two networks P and Q , we say that Q is *denser* than P if $\tilde{Q}(d)$ FOSD $\tilde{P}(d)$, that is, if

$$\sum_{d=0}^D \tilde{Q}(d)f(d) \geq \sum_{d=0}^D \tilde{P}(d)f(d) \quad \text{for any nondecreasing function } f \text{ of } d. \quad (\text{A.13})$$

We regard higher mobile phone coverage precisely as corresponding to a FOSD shift in \tilde{P} .

From (A.8), (A.9), and (A.10) it follows that a deterioration in economic conditions leads to a larger increase in the fraction of people protesting in denser (Q) compared to less dense (P) networks. In formula form,

$$-\frac{d\bar{y}^Q}{d\Delta\text{GDP}} \geq -\frac{d\bar{y}^P}{d\Delta\text{GDP}}. \quad (\text{A.14})$$

To see this note that from equation (A.8), $-\frac{d\bar{y}}{d\Delta\text{GDP}} = \frac{-\sum_{d=1}^D \tilde{P}(d) \frac{\partial H(\cdot)}{\partial \Delta\text{GDP}}}{1 - \sum_{d=1}^D \tilde{P}(d) \frac{\partial H(\cdot)}{\partial y}}$. Under assumptions (A.9) and (A.10), as the density of the network increases, the numerator increases, while the denominator decreases, so that (A.14) holds.

The intuition for this result has to do with the larger share of connected agents in denser networks. If individuals with more connections are more likely to increase their partici-

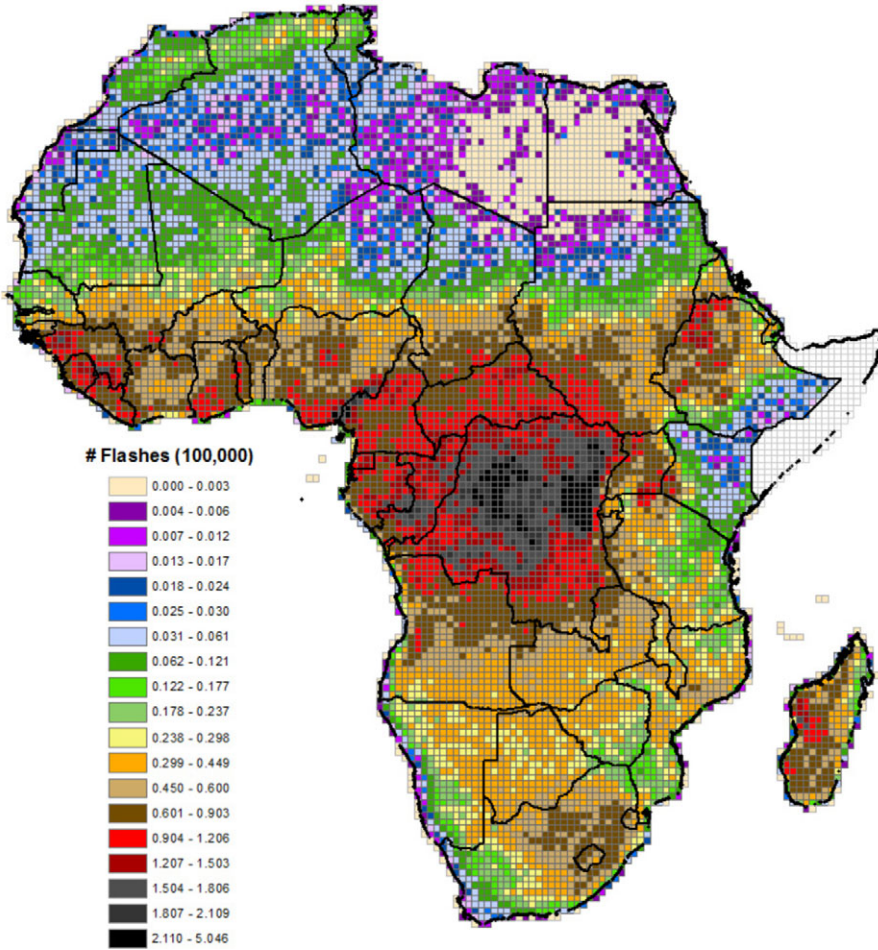


FIGURE A.3.—Lightning strikes in Africa. The figure reports the average number of lightning strikes between 1995 and 2010 in each $0.5^\circ \times 0.5^\circ$ degree cell. Source: NASA.

pation when the economy deteriorates (equation (A.9)), then worse economic conditions will directly lead to greater protest participation in denser networks. This is a compositional effect.

In this setting, though, every individual will know that each individual's propensity to participate has increased and that others know it, and this effect is greater in denser networks. Once more, this effect works through strategic complementarities and further magnifies the effect of recessions on protest participation in denser networks.

A.1.5. From Theory to the Empirical Model

The previous model provides testable implications that can be brought to the data. Let us denote by d_i a dummy equal to 1 if an individual uses a mobile phone and let \bar{d} denote the fraction of individuals with mobile phones in the population.

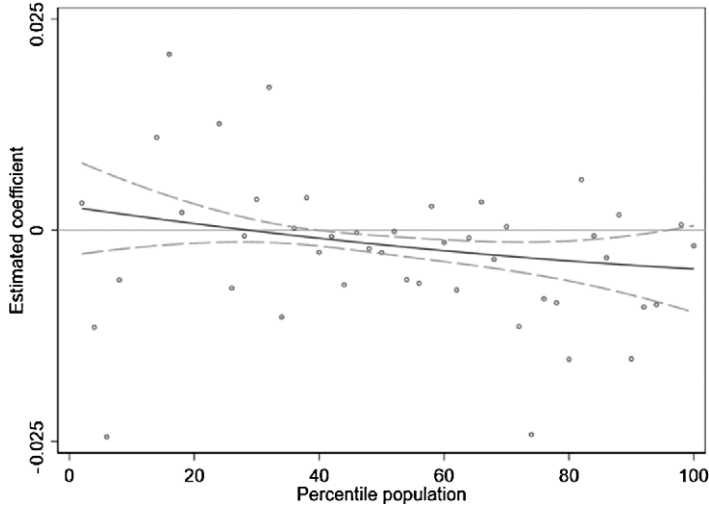


FIGURE A.4.—First-stage estimates at different levels of population: compliers. The figure reports the effect of the interaction between Z and ΔGDP on the interaction between coverage and ΔGDP (the parameter θ_2 in equation (3) in the paper) separately by pairs of percentiles (1–2, 3–4, ..., 99–100) of the distribution of population. Point estimates are reported in the figures as dots. We superimpose a quadratic fit where each observation is weighted by the inverse of the square of the standard error of the associated estimate. The graph reports this estimated regression curve as well as the 95 percent confidence interval around the prediction.

Linearizing equations (A.6), (A.7), (A.11), and (A.12) one can derive the expression for individual i 's participation,

$$y_i = \gamma_0 + \gamma_1 d_i + \gamma_2 \Delta\text{GDP} d_i + \gamma_3 \bar{y} + \gamma_4 \bar{y} d_i + \gamma_5 \Delta\text{GDP} + u_i, \quad (\text{A.15})$$

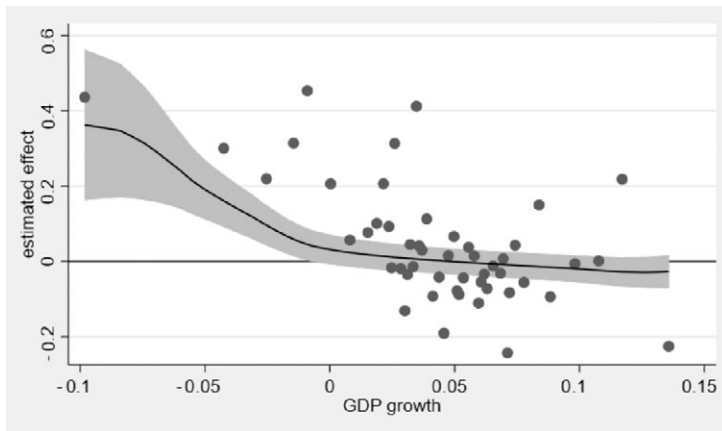


FIGURE A.5.—The effect of coverage on protests at different levels of GDP growth: OLS. The figure reports the effect of coverage on protests by percentile of the ΔGDP distribution, estimated nonparametrically. The OLS estimates refer to 50 groups of two percentiles (1–2, 3–4, ..., 99–100). Point estimates are reported in the figures as dots. We superimpose a kernel-weighted local polynomial regression where each observation is weighted by the inverse of the square of the standard error of the associated estimate using a minimum distance estimator. We use a polynomial of degree 0 and an Epanechnikov kernel function, with a rule-of-thumb bandwidth. The graph reports this estimated regression curve as well as the 95 percent confidence interval around the prediction.

TABLE A.I
CELL-LEVEL COVARIATES

Variable	Source	Short Description
Population	SEDAC/NASA	Population size for each cell, extracted from the Gridded Population of the World, v.3. Data are available for 1990, 1995, 2000, and 2005. We obtain the remaining years by linear interpolation.
Cities (number)	SEDAC/NASA	Number of cities in the cell at year 2000, calculated in GIS from the Global Rural–Urban Mapping Project, v.1.
Capital (dummy)	Natural Earth	Capital cities are identified from Natural Earth, a data set of populated places that includes geographical information on the location of all capital cities worldwide.
Border distance (100 km) Capital distance (100 km) Coast distance (100 km)	Authors' calculations	All distances are calculated in GIS from the cell centroid. Border distance is to the nearest neighboring country, regardless of whether this is located across international waters; capital distance is to the national capital city; coast distance is to the nearest coast.
Primary roads (100 km)	Africa Infrastructure Country diagnostic (ADB)	Georeferenced road files are downloaded separately for each country. Data usually refer to network in 2007, and are discussed in Gwilliam, Foster, Archondo-Callao, Briceño-Garmendia, Nogales, and Sethi (2008). For each cell we calculate the road network in GIS. Country-specific files are not available for North African countries. In this case, data are obtained from the Roads of Africa data set.
Electricity (100 km)	Africa Infrastructure Country diagnostic (ADB)	Georeferenced electricity files are available from the ADB data set for all countries, except Egypt, Libya, and Morocco. For these countries, data are obtained from the OpenStreetMap project. Data usually refer to the network in 2007. For each cell we calculate the electricity network in GIS.
Infant mortality rate (‰)	SEDAC/NASA	The cell-specific infant mortality rate is based on raster data from the Global Poverty Mapping project. The variable is the average pixel value inside the grid cell. The unit is the number of children per 10,000 that die before reaching their first birthday. The indicator refers to the year 2000.
Mountain (%)	UNEP-WCMC	Share of mountainous terrain within each cell. This indicator is based on high-resolution mountain raster data from the UNEP's Mountain Watch Report 2002.
Forest (%)	GlobCover	Share of forest cover in a cell, extracted from the GlobCover 2009 data set. We follow the FAO land cover classification and aggregate land classes equal to 40, 50, 60, 70, 90, 100, 110, 160, and 170.

(Continues)

where y_i is a dummy for individual i participating in a protest and u is an error term. This is equation (4) in the paper. If assumptions (A.1), (A.2), (A.9), and (A.10) hold, we expect $\gamma_2 \leq 0$, $\gamma_5 \leq 0$, $\gamma_3 \geq 0$, and $\gamma_4 \geq 0$.

Solving for \bar{y} , it follows that

$$\bar{y} = \beta_0 + \beta_1 \bar{d} + \beta_2 \Delta \text{GDP} \bar{d} + \beta_3 \Delta \text{GDP} + u, \quad (\text{A.16})$$

TABLE A.I—Continued

Variable	Source	Short Description
Night lights	NOAA/NASA	Night lights are cloud-free composites from version 4 of the DMSP-OLS Nighttime lights time series data set. For each cell, we calculate in GIS the average light intensity of all pixels in the cell. In years where more than one satellite was available, we calculate the average intensity from the two. To obtain the variables used in the analysis we follow Henderson, Storeygard, and Weil (2012) and we compute 3-years moving averages, replacing night lights with zeros in the presence of gas flares. Following Michalopoulos and Papaioannou (2013), we focus on the log of night lights, adding a small number (0.01) to deal with zeros.
Diamonds (dummy)	PRIO	The variable includes any site with known activity, meaning production or confirmed discovery from the Diamond Resources data set. For each cell we calculate the presence of a diamond mine in GIS.
Oil (%)	PRIO	The Petroleum Data Set groups oil fields in polygons within a buffer distance of 30 km. For each cell we calculate the percentage that is covered by an oil field in GIS.
Mines (dummy)	U.S. Geological Survey	For each cell we calculate the presence of a mine in GIS, irrespective of the type of mineral and magnitude of production.
Temperature (Celsius)	NOAA/NASA	Yearly mean temperature in the cell based on monthly meteorological statistics from the GHCN_CAMS Gridded 2 m data set of the National Oceanic and Atmospheric Administration (NOAA 2011).
Rainfall (m)	GPCP	Total amount of yearly rainfall in the cell based on monthly meteorological statistics from the GPCP v.2.2 Combined Rainfall Data Set.
Lightning strikes (per km ² per year)	GHRC/NASA	Data refer to lightning activity calculated from the Optical Transient Detector (OTD) and the Lightning Imaging Sensor (LIS). Each lightning strike is recorded along with its spatial location, with a level of resolution of 5–10 km on the ground. We use the LIS/OTD 0.5 Degree High Resolution Full Climatology (HRFC), which calculates the average lightning density in 0.5° × 0.5° cells over the period 1995–2010.

where $\beta_k \approx \frac{\gamma_k}{1-\gamma_3-\gamma_4\bar{d}}$, $k = 1, 2$, and for the equilibrium to be stable we expect $\gamma_3 + \gamma_4\bar{d} < 1$ (this is effectively equation (A.5)). Assuming for simplicity that the fraction of individuals using a mobile phone (\bar{d}) is identical to the fraction of people in reach of the signal (Cov), this gives

$$\bar{y} = \beta_0 + \beta_1 \text{Cov} + \beta_2 \Delta \text{GDPCov} + \beta_3 \Delta \text{GDP} + u. \quad (\text{A.17})$$

This gives the aggregate model (1) in the paper.¹ Equation (A.16) (respectively, (A.17)) says that the fraction of individuals protesting in the economy or, equivalently, the num-

¹Alternatively, let $\bar{d} = \kappa_0 + \kappa_1 \text{Cov} + \tau$. In this case, $\beta_k \approx \frac{\gamma_k \kappa_1}{1-\gamma_3-\gamma_4\bar{d}}$ for $k = 1, 2$.

TABLE A.II
DESCRIPTIVE STATISTICS: CELL CHARACTERISTICS^a

	Avg.	Std. Dev.	Min.	Max.
Mobile phone coverage (%)	0.43	0.42	0	1
Protests per 100,000 pop.: GDELT	1.33	11.55	0	48,000
Protests per 100,000 pop.: ACLED	0.09	1.49	0	20,000
Protests per 100,000 pop.: SCAD	0.06	1.84	0	10,811
Population (1000s)	84.35	265.46	1	12,866
Country GDP growth	0.05	0.04	-0.33	0.63
Border distance (100 km)	1.97	2.11	0	25.51
Night lights	4.55	10.32	0.01	61.58
Oil (percent)	0.06	0.20	0	1
Mines (dummy)	0.22	0.41	0	1
Diamonds	0.03	0.18	0	1
Forest (%)	0.24	0.26	0	1
Mountain (%)	0.24	0.32	0	1
Infant mortality rate (‰)	8.31	3.72	0.84	18.29
Cities	2.37	3.86	0	35
Capital city (dummy)	0.07	0.26	0	1
Distance to capital (100 km)	3.83	3.38	0.05	31.31
Distance to coast (100 km)	4.46	3.96	0	18.01
Electricity (100 km)	0.47	0.48	0	1.96
Primary Roads (100 km)	1.40	1.34	0	6.37
Lightning strikes (100,000)	0.53	0.42	0	5.02
Rainfall (m)	0.98	0.57	0	3.28
Temperature (Celsius)	23.37	4.19	5.01	38.76

^aThe table reports descriptive statistics for each of the 10,409 cells of $0.5^\circ \times 0.5^\circ$ degree resolution. All data, except population in the fifth row, are weighted by cell population. The first row reports the fraction of the population in reach of mobile phone signal. The second, third and fourth rows report the average number of protests in a year per 100,000 people, from GDELT, ACLED, and SCAD respectively. The sixth row reports the country's yearly growth in GDP per capita. The remaining rows report cross-sectional physical, climatic, geographical, and socioeconomic characteristics of each cell. Table A.I reports the definitions as well as the sources of each of these variables.

TABLE A.III
MOBILE PHONES AND PROTESTS: OLS^a

	Protests: GDELT		Protests: ACLED		Protests: SCAD	
	(1)	(2)	(3)	(4)	(5)	(6)
Coverage	0.015	0.118	0.002	0.024	0.021	0.052
	[0.66]	[0.05]	[0.84]	[0.40]	[0.09]	[0.01]
Δ GDP \times coverage		-1.988		-0.420		-0.599
		[0.02]		[0.36]		[0.01]
Observations	150,883	150,883	150,883	150,883	150,883	150,883

^aThe table reports OLS estimates of equation (1) in the paper, based on GDELT, ACLED, and SCAD, respectively. All specifications include cell and country \times year fixed effects, plus the time-varying controls log population, log rainfall, log temperature, and log night lights plus the interaction between a linear time trend and the cross-sectional cell characteristics fraction of the cell's area covered by mountains and forests, oilfields, presence of mineral and diamond mines, latitude and longitude of the cell centroid, cell area, distance of the centroid to the coast and whether the cell is on the coast, whether the cell hosts the country's capital, distance to capital, whether on the border and distance to the border, number of cities in the cell, dummies for first-order administrative division the majority of the cell belongs to, kilometers of primary roads, kilometers of electrical grid, infant mortality rate, and dummies for missing values of all these variables. Summary statistics for these variables are reported in Table A.II, while Table A.I reports their definitions and original sources. All regressions are weighted by cell population. The p -values for wild cluster bootstrap standard errors at the level of country are reported below each coefficient. See also the notes to Table I in the paper.

TABLE A.IV
LIGHTNING STRIKES AND LOCAL ECONOMIC DEVELOPMENT^a

	Night Lights Growth (1)	Population (2)	Desertification (3)
Z	-0.001 [0.93]	-0.001 [0.75]	0.001 [0.60]
$\Delta\text{GDP} \times Z$	-0.009 [0.65]	-0.002 [0.52]	-0.021 [0.21]
Observations	150,883	150,883	150,883

^aThe table reports OLS estimates of regressions of a number of variables on the instruments (Z and $\Delta\text{GDP} \times Z$). The dependent variable in column 1 is the growth rate in night lights intensity, as defined in Table A.I. The dependent variable in column 2 is log population, while in column 3 it is a dummy for desertification. The latter is based on values of the Normalized Difference Vegetation Index (Tucker (1979)) between 0 and 0.2. All regressions include cell and country \times year fixed effects plus the entire set of cell-level controls described in the notes to Table I in the paper, with the exclusion of the variable log population in columns 2 and 3. All regressions are weighted by cell population. The p -values for wild cluster bootstrap standard errors at the level of country are reported below each coefficient. See also notes to Table I in the paper.

ber of protests, which we take as a monotonic transformation of this fraction, is a negative function of GDP growth, a positive function of the fraction of those connected (respectively, mobile phone coverage), and a negative function of the interaction between these two variables.

Estimates of the aggregate equation are unable to provide information on the “structural parameters” of the microfunded model of behavior. However, these parameters can be identified based on the micromodel (A.15). This model will allow identification of the extent to which the enhancing effect of connectivity on protests during bad economic times ($\beta_2 < 0$) is due to greater responsiveness to economic conditions among those connected ($\gamma_2 < 0$) or to their greater responsiveness to their peers’ participation ($\gamma_4 > 0$).

Identification of model (A.15) involves some challenges though. Even ignoring the possibility of nonrandom allocation of mobile phones across areas and individuals, estimates of model (A.15) will still be potentially plagued by a classical reflexivity problem (Manski (1993)). However, equation (A.16) suggests that one can obtain consistent estimates of the parameters in (A.15) by instrumenting average participation in the economy \bar{y} (and its interaction with mobile phone use d_i) with mobile phone coverage \bar{d} and its interac-

TABLE A.V
MOBILE PHONES AND PROTESTS DURING LOW-LIGHTNING MONTHS: 2SLS^a

	GDELT (1)	ACLED (2)	SCAD (3)
Coverage	-0.175 [0.44]	0.036 [0.78]	-0.099 [0.21]
$\Delta\text{GDP} \times \text{coverage}$	-3.755 [0.06]	-0.774 [0.05]	-0.592 [0.10]
Observations	150,883	150,883	150,883

^aThe table reports 2SLS estimates of equation (1) in the paper for protests occurring during months when lightning intensity is at its lowest (June, July, and August for countries south of the Equator; December, January, and February for countries north of the Equator; see Christian et al. (2003)). All specifications include cell and country \times year fixed effects, plus the entire set of cell-level controls described in notes to Table I in the paper. All regressions are weighted by cell population. The p -values for wild cluster bootstrap standard errors at the level of country are reported below each coefficient. See also notes to Table I in the paper.

TABLE A.VI
MOBILE PHONES AND PROTESTS: 2SLS—ALTERNATIVE CLUSTERING OF STANDARD ERRORS^a

	GDELTA (1)	ACLED (2)	SCAD (3)
Coverage	-0.493	0.063	-0.062
Country	[0.23]	[0.84]	[0.68]
Admin1 and country × year (two-way)	[0.49]	[0.85]	[0.74]
Admin1	[0.50]	[0.82]	[0.72]
Admin2 and country × year(two-way)	[0.63]	[0.84]	[0.73]
Admin2	[0.64]	[0.75]	[0.69]
IM 91.7%	[-1.793; 0.593]	[-0.413; 0.370]	[-0.363; 0.136]
ΔGDP × coverage	-5.776	-2.151	-1.886
Country	[0.05]	[0.04]	[0.05]
Admin1 and country × year (two-way)	[0.03]	[0.08]	[0.02]
Admin1	[0.03]	[0.08]	[0.02]
Admin2 and country × year(two-way)	[0.02]	[0.06]	[0.01]
Admin2	[0.01]	[0.04]	[0.01]
IM 91.7%	[-9.754; -0.540] ^a	[-2.677; -0.037] ^a	[-10.002; 6.577]
Observations	150,883	150,883	150,883

^aThe table reports the p -values associated to the same specification as in columns 4, 6, and 8 of Table I in the paper with different clustering of the standard errors, respectively, clustered by country, two-way clustering by first-order administrative division and country × year, first-order administrative division, second-order administrative division and country × year, and second-order administrative division. The 91.7% Ibragimov and Müller (2016) confidence intervals also reported. The superscript “a” denotes that the confidence interval does not include zero. See also notes to Table I in the paper.

tion with GDP growth (as well as their interaction with mobile phone use d_i). Intuitively, and conditional on d_i , the fraction of those covered in society \bar{d} will only matter for individual participation through the spillover effect. This is the approach that we follow in Section 5.2 and that we apply empirically in Section 6.4.

A.1.6. *The Role of Enhanced Information and Enhanced Coordination*

We separate the effect of enhanced information (a decrease in γ_2) from the effect of enhanced coordination (an increase in γ_4) as follows. Using a Taylor expansion around $\gamma_2 = \gamma_4 = 0$, $\beta_2 \approx A\gamma_2 + B\gamma_4$, where $A = \frac{1}{(1-\gamma_3-\gamma_4\bar{d})}$ and $B = -\frac{\gamma_2\bar{d}}{(1-\gamma_3-\gamma_4\bar{d})^2}$. The contribution of coordination relative to information is hence $\frac{B}{A} = -\frac{\gamma_2\bar{d}}{(1-\gamma_3-\gamma_4\bar{d})}$. Using the model estimates in column 3 of Table V, this is $\frac{0.217 \times 0.71}{1 - 0.577 - 0.295 \times 0.71} = 0.72$, implying that around 42 percent of the effect is due to increased coordination and 58 percent is due to increased information.

A.2. *Technical Information on Lightning Strikes and Their Effect on Mobile Phone Communication*

In the paper we use the interaction between average lightning strikes in a cell and a linear time trend as an instrument for mobile phone coverage. We claim that lightning strikes deter the adoption of mobile phone technology as it becomes available, by both raising the cost of installing telecommunication equipment and by negatively affecting its functionality. In this section we provide background information on the sources of data on lightning strikes and their effect on mobile phone functionality.

TABLE A.VII
ROBUSTNESS CHECKS—ALTERNATIVE FUNCTIONAL FORMS: 2SLS^a

	Trimmed (1)	Winsorized (2)	Square Root (3)	Levels (4)
GDELТ				
Coverage	-0.911 [0.07]	-0.690 [0.10]	-0.522 [0.49]	6.244 [0.62]
$\Delta\text{GDP} \times \text{coverage}$	-4.807 [0.10]	-4.991 [0.08]	-12.326 [0.03]	-137.683 [0.01]
Observations	149,567	150,883	150,883	150,883
$\text{SW } F - Z$	12.600	11.580	11.580	11.580
$\text{SW } F - \Delta\text{GDP} \times Z$	5.154	6.968	6.968	6.968
ACLED				
Coverage	0.254 [0.18]	0.074 [0.75]	0.024 [0.97]	0.306 [0.67]
$\Delta\text{GDP} \times \text{coverage}$	-2.196 [0.03]	-1.651 [0.01]	-2.790 [0.04]	-5.737 [0.01]
Observations	149,470	150,883	150,883	150,883
$\text{SW } F - Z$	13.890	11.580	11.580	11.580
$\text{SW } F - \Delta\text{GDP} \times Z$	5.383	6.968	6.968	6.968
SCAD				
Coverage	-0.051 [0.65]	-0.069 [0.51]	-0.090 [0.61]	0.122 [0.76]
$\Delta\text{GDP} \times \text{coverage}$	-1.020 [0.06]	-1.024 [0.03]	-2.607 [0.02]	-3.988 [0.01]
Observations	149,483	150,883	150,883	150,883
$\text{SW } F - Z$	12.160	11.580	11.580	11.580
$\text{SW } F - \Delta\text{GDP} \times Z$	4.917	6.968	6.968	6.968

^aThe table reports 2SLS estimates of equation (1) in the paper. The upper panel refers to GDELТ, the middle panel to ACLED, and the lower panel to SCAD. All specifications include cell and country \times year fixed effects, plus the entire set of cell-level controls described in notes to Table I in the paper. In columns 1 and 2 the dependent variable is trimmed and winsorized at the 99th percentile, respectively. In column 3 the dependent variable is the square root of the number of protests per capita. In column 4 the dependent variable is the number of protests per capita. The p -values for wild cluster bootstrap standard errors at the level of country are reported below each coefficient. See also notes to Table I in the paper.

Lightning strikes are recorded by the Optical Transient Detector (OTD), a space-borne optical sensor operating between April 1995 and March 2000, and its successor, the Lightning Imaging Sensor (LIS), launched in November 1997 and operating until April 2015. Both OTD and LIS are onboard satellites in low Earth orbit, viewing an Earth location for 3 and 1.5 minutes, respectively, as they passed overhead. OTD completed 14 orbits/day while LIS completed 16 orbits/day. Lightning strikes are recorded along with their spatial location (latitude, longitude) with a level of resolution of at least 10 km on the ground. For each $0.5^\circ \times 0.5^\circ$ grid cell, the total view time (observation duration) and flash count are summed over all orbits. Flash counts are scaled by each instrument's detection efficiency, which varies with the time of day (and geographic location, in the case of the OTD). We ultimately obtain the combined measure of lightning strike intensity (lightning strikes per kilometer squared per year) by dividing the total scaled flash counts from both the LIS and the OTD by the total view time over the year.

Lightning strikes impact mobile phone functionality mostly by inducing overvoltages and overcurrents in the electronic hardware of the base transceiver station (BTS), the cru-

TABLE A.VIII
ALTERNATIVE MEASURES OF ECONOMIC GROWTH—NIGHT LIGHTS: 2SLS^a

	(1)	(2)	(3)
		GDELTA	
Coverage	-0.669 [0.18]	-0.764 [0.17]	-0.690 [0.18]
National growth × coverage	-2.236 [0.08]		-2.666 [0.20]
Regional growth × coverage		-0.772 [0.39]	0.429 [0.75]
		ACLED	
Coverage	0.047 [0.89]	0.044 [0.91]	0.069 [0.85]
National growth × coverage	-1.359 [0.19]		-0.898 [0.10]
Regional growth × coverage		-0.863 [0.14]	-0.459 [0.28]
		SCAD	
Coverage	-0.093 [0.50]	-0.110 [0.42]	-0.086 [0.54]
National growth × coverage	-1.007 [0.06]		-0.854 [0.28]
Regional growth × coverage		-0.537 [0.08]	-0.153 [0.59]
SW coverage	2.728	2.518	3.404
SW national growth × coverage	40.290		125.84
SW regional growth × coverage		12.171	13.839
Observations	149,110	149,110	149,110

^aThe table reports 2SLS estimates of equation (1) in the paper where Δ GDP is replaced by the growth rate in night lights. All specifications include cell and first-order administrative division × year effects plus the entire set of cell-level controls described in notes to Table I in the paper. Specifications in column 2 include the first-order administrative division growth rate in night lights interacted with coverage. Column 3 includes both regressors. All regressions are weighted by cell population. The *p*-values for wild cluster bootstrap standard errors at the level of country are reported in parentheses. See also notes to Table I in the paper.

cial piece of equipment enabling wireless communication between mobile phones. There are three main mechanisms through which lightning strikes damage BTS (ITU (1996)). First, lightning strikes generate currents distributed among power supply cables, inducing overvoltages proportional to the transfer impedance between the cable shield and the core (resistive coupling). Second, they induce magnetic field variations producing voltages and currents in the internal wiring and in the outdoor cable plant (magnetic coupling). Finally, they generate electromagnetic fields, which impress substantial overvoltages on the telecommunication network, interfering with the equipment interface (electromagnetic coupling). While the use of high antenna masts for wireless communication has significantly increased the risk for damages due to direct lightning strikes to the site, strikes do not need to directly hit the BTS in order to damage it. Induction hits caused by lightning strikes near the tower cause the electrons in the cables to move away from the strike, creating current on the lines.

Either type of strike will usually destroy unprotected equipment. The consequences in terms of service disruption range from permanent—when direct lightning strikes provoke fire, explosion or other physical destruction to the BTS—to shorter service interruptions,

TABLE A.IX
FIRST-STAGE ESTIMATES: AFROBAROMETER^a

	% Participating (1)	% Participating × Mobile (2)
% mobile	0.025 [0.08]	−0.040 [0.06]
Δ GDP × % mobile	−0.710 [0.11]	0.146 [0.70]
% mobile × mobile	0.009 [0.29]	0.127 [0.01]
Δ GDP × % mobile × mobile	−0.054 [0.75]	−1.424 [0.01]
Observations	73,781	73,781

^aThe table reports first-stage estimates underlying the 2SLS estimates of equation (4) reported in column 1 of Table V in the paper. All regressions are weighted by sampling weights. The *p*-values for wild cluster bootstrap standard errors at the level of country are reported in parentheses. See also notes to Table V in the paper.

depending on the severity of the hit. The U.S. army estimates that it would take between 10 and 30 days to repair communication equipment critically hit by a lightning strike (Tobias (1993)). The repair time is likely to take much longer in the African context.

Protection procedures against lightning strikes include earthing, bonding, shielding, and installation of surge protective devices. In all cases, these procedures do not offer full protection, and the probability of a strike damaging the equipment remains nonnegligible. Our best estimate of the cost of lightning protection, based on a number of technical reports and industry white papers (Rahaman (2009), MTN (2013)), is on the order of 15 percent of the cost of tower installation. This cost is nonnegligible and will have obvious negative consequences on the decision to install a tower, as this will ex ante deter firms and consumers from investing in this technology.

REFERENCES

- CHRISTIAN, H. J., R. J. BLAKESLEE, D. J. BOCCIPPIO, W. L. BOECK, D. E. BUECHLER, K. T. DRISCOLL, S. J. GOODMAN, J. M. HALL, W. J. KOSHAK, D. M. MACH et al. (2003): “Global Frequency and Distribution of Lightning as Observed From Space by the Optical Transient Detector,” *Journal of Geophysical Research: Atmospheres*, 108 (D1), ACL-4. [11]
- GRANOVETTER, M. (1978): “Threshold Models of Collective Behavior,” *American Journal of Sociology*, 84 (6), 1420–1443. [1]
- GWILLIAM, K., V. FOSTER, R. ARCHONDO-CALLAO, C. BRICEÑO-GARMENDIA, A. NOGALES, AND K. SETHI (2008): “The Burden of Maintenance: Roads in Sub-Saharan Africa,” AICD Background Paper (No. 14). [8]
- HENDERSON, J.V., A. STOREYGARD, AND D. N. WEIL (2012): “Measuring Economic Growth from Outer Space,” *American Economic Review*, 102 (2), 994–1028. [9]
- IBRAGIMOV, R., AND U. K. MÜLLER (2016): “Inference with Few Heterogeneous Clusters,” *Review of Economics and Statistics*, 98 (1), 83–96. [12]
- ITU (1996): *K.39—Series K: Risk Assessment of Damages to Telecommunication Sites due to Lightning Discharges*. ICT Data and Statistics. Division Telecommunication Development Bureau, International Telecommunication Union. [14]
- JACKSON, M. O., AND L. YARIV (2007): “Diffusion of Behavior and Equilibrium Properties in Network Games,” *American Economic Review*, 97 (2), 92–98. [1,2]
- MANSKI, C. F. (1993): “Identification of Endogenous Social Effects: The Reflection Problem,” *The Review of Economic Studies*, 60 (3), 531–542. [11]

- MICHALOPOULOS, S., AND E. PAPAIOANNOU (2013): "National Institutions and Subnational Development in Africa," *The Quarterly Journal of Economics*, 129 (1), 151–213. [9]
- MTN (2013): "MTN Group Limited Integrated Report for the Year Ended 31 December 2013," available at <https://www.mtn.com/wp-content/uploads/2019/02/AR-Booklet-2013.pdf>. [15]
- RAHAMAN, A. (2009): "Lightning Protection Practices in Bangladesh: An Overview," NAM S&T Centre's Publication on: Lightning Protection. [15]
- TOBIAS, J. M. (1993): "Lightning Protection System Design: Applications for Tactical Communications Systems," Technical report, U.S. Army Communications-Electronics Command. [15]
- TUCKER, C. J. (1979): "Red and Photographic Infrared Linear Combinations for Monitoring Vegetation," *Remote sensing of Environment*, 8 (2), 127–150. [11]

Co-editor Fabrizio Zilibotti handled this manuscript.

Manuscript received 11 May, 2016; final version accepted 12 October, 2019; available online 19 December, 2019.